

RESEARCH ARTICLE | SEPTEMBER 19 2023

Non-uniform Gd distribution and magnetization profiles within GdCoFe alloy thin films

Special Collection: [Ferrimagnetic Spintronics](#)

O. Inyang ; C. Swindells ; D. Rianto ; L. Bouchenoire ; R. J. H. Morris ; A. Merkulov ; A. Caruana ; C. Kinane ; T. P. A. Hase ; D. Atkinson



Appl. Phys. Lett. 123, 122403 (2023)
<https://doi.org/10.1063/5.0165423>

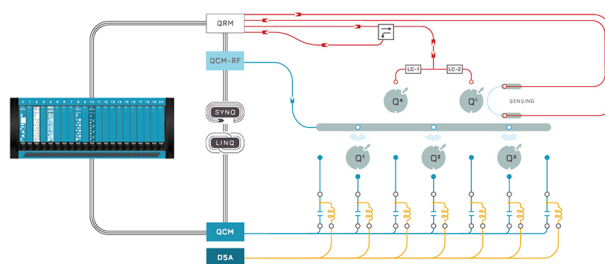


CrossMark

QBLOX

Integrates all Instrumentation + Software for Control and Readout of

Superconducting Qubits
NV-Centers
Spin Qubits



Spin Qubits Setup

[find out more >](#)

Non-uniform Gd distribution and magnetization profiles within GdCoFe alloy thin films

Cite as: Appl. Phys. Lett. **123**, 122403 (2023); doi: [10.1063/5.0165423](https://doi.org/10.1063/5.0165423)

Submitted: 28 June 2023 · Accepted: 4 September 2023 ·

Published Online: 19 September 2023



View Online



Export Citation



CrossMark

O. Inyang,¹ C. Swindells,² D. Rianto,¹ L. Bouchenoire,^{3,4} R. J. H. Morris,⁵ A. Merkulov,⁵ A. Caruana,⁶ C. Kinane,⁶ T. P. A. Hase,⁷ and D. Atkinson^{1,a)}

AFFILIATIONS

¹Department of Physics, Durham University, Durham DH1 3LE, United Kingdom

²Department of Materials Science and Engineering, University of Sheffield, Sheffield S1 3JD, United Kingdom

³XMaS, The UK-CRG Beamline, ESRF, 71 Avenue des Martyrs, CS 40220, Grenoble F-38043, France

⁴Department of Physics, University of Liverpool, Liverpool L69 7ZE, United Kingdom

⁵IMEC, Kapeldreef 75, Leuven 3001, Belgium

⁶ISIS Neutron and Muon Source, Rutherford Appleton Lab, Oxfordshire OX11 0QX, United Kingdom

⁷Department of Physics, University of Warwick, Coventry CV4 7AL, United Kingdom

Note: This paper is part of the APL Special Collection on Ferrimagnetic Spintronics.

^{a)}Author to whom correspondence should be addressed: del.atkinson@durham.ac.uk

ABSTRACT

Rare earth (RE):transition metal (TM) ferrimagnetic alloys continue to attract significant attention for spintronics. This work focuses on the elemental distribution of RE and TM elements throughout the thickness of nominally uniform films and the resulting spatial variations of the magnetization within these layers. Samples of CoFe alloyed with Gd were studied using secondary ion mass spectroscopy, polarized neutron reflectometry, and x-ray resonant magnetic reflectivity. The samples were grown by magnetron co-sputtering to control the RE:TM alloy ratio of the ferrimagnetic layer, which was combined with W and Pt layers as either under or over-layers to create sample structures such as W/Gd_x(Co₇₀Fe₃₀)_{100-x}/Pt, where $x = 0, 8, \text{ and } 23$ at. %. Results show that uniformly deposited thin-films have a significant variation in the distribution of the TM and RE through the film thickness, and this leads to a spatial distribution in the net magnetization profile and a non-uniform Gd magnetization profile within the layer. These findings have implications for the application RE:TM alloys in spintronics as they may impact the perpendicular magnetic anisotropy, the ferrimagnetic compensation temperature, and interfacial spin transport.

© 2023 Author(s). All article content, except where otherwise noted, is licensed under a Creative Commons Attribution (CC BY) license (<http://creativecommons.org/licenses/by/4.0/>). <https://doi.org/10.1063/5.0165423>

Amorphous thin-film ferrimagnetic alloys, which combine rare-earth and transition metals (RM:TM), have provided exceptional physical insight and significant interest for applications for more than 50 years. Early studies were focused on the occurrence of a perpendicular magnetic anisotropy (PMA) and the associated magnetic domain structure,¹⁻³ the origin of the growth-induced PMA,⁴⁻⁹ and the large anomalous Hall effect.^{10,11} With a favorable combination of properties, these ferrimagnetic alloys emerged as materials for applications, being initially considered as an alternative to ferrimagnetic crystalline garnets for bubble memory^{1,12} and more significantly developed as the recording media for magneto-optical data storage.¹³⁻¹⁵ This latter application underpinned much of the research on RE:TM alloys over the following years, see, for example, Refs. 16 and 17. More recently, the combination of PMA and the presence of compensation effects

has attracted attention for spintronic applications, see recent reviews.¹⁸⁻²⁰ Compensation in RE:TM alloys results from the different temperature dependencies of the magnetization and the angular momentum of the RE and TM sub-lattices. As the coupling between the RE and TM is antiferromagnetic, the net magnetization will fall to zero when the moments of the RE and TM lattices are equal at a temperature, T_M . Likewise, the net angular momentum will also vanish at T_A .²¹⁻²³ The compensation temperatures necessarily depend upon the alloy composition.

Spintronic studies have addressed the physics of spin angular momentum transfer in antiferromagnetically coupled systems, the efficiency of the spin-orbit torque (SOT) switching,²⁴⁻³⁰ the influence of the ferrimagnetic compensation on domain wall velocity, skyrmions dynamics, and the skyrmion Hall effect.³¹⁻³⁴ Recent research has

focused on understanding the spin transport and magnetization of RE:TM ferrimagnetic alloys with less significance attached to any structural/compositional issues. However, it has emerged recently that within a given RE:TM thin-film, the distribution of the constituent atomic species may be inhomogeneous. It has been suggested that segregation of RE atoms may occur at the surface³⁵ or through solid state diffusion leading to the coexistence of different phases³⁶ within the film. Since the magnetic properties are derived from exchange interactions at the local level, any inhomogeneity will lead to complex magnetic behavior,³⁷ magnetic sensitivity to local concentration,³⁵ and behavior that can change over time.³⁸

Intentional spatial variation in the composition has been used to control the anisotropy, modify the domain structure,³⁹ and break the magnetization symmetry to enable field-free SOT switching⁴⁰ in thin films. However, naturally occurring spatial variation through the film thickness, which may have significant consequences for the spintronic behavior, has been less well documented. For example, a local reduction in RE content may change the structure from amorphous to crystalline,⁴¹ while a distribution of compensation temperatures through the thickness will reduce the benefits associated with single point compensation. For many spintronic applications, it is the interfaces of the ferrimagnetic alloy with non-magnetic layers such as Pt and W that are vital.⁴² Any compositional variations at these interfaces will change the electronic structure at the interface that may directly affect the interfacial spin-transport,^{43–46} spin-orbit coupling across the interface,^{47,48} the interfacial Dzyaloshinskii–Moriya interaction (DMI),^{49–51} and proximity induced magnetization (PIM),^{52–55} which has been linked to interfacial spin transport.^{56–58}

This study explored the elemental composition distributions and magnetization profiles through the film thickness of uniformly sputter-deposited GdCoFe thin-films, which are commonly used for RE:TM spintronics.^{18–20} The RE:TM films were layered with Pt and W, which are important non-magnetic layers in spintronics^{59–62} and ensure any buffer-induced structural changes are consistent with applications.

Samples were deposited by magnetron sputtering onto oxidized Si substrates, from a base pressure of 10^{-7} Torr, with high purity Ar as the sputtering gas at a deposition pressure of 3×10^{-3} Torr. Thin-films of GdCoFe alloys were grown by deposition-rate calibrated co-sputtering from Gd and CoFe targets to tune the RE:TM alloy composition. All sample depositions were done at room temperature, and there was no heat treatment after deposition. The deposition rate of the individual targets was first calibrated using x-ray reflectivity (XRR). The average composition ratio of the RE:TM layer was confirmed with energy dispersive x-ray spectroscopy (EDX). The RE:TM films were investigated with the Gd content of 0, 8, and 23 at.% in order to explore the effect of the Gd content, which determines the onset of the amorphous structure in these alloys.⁴¹ The nominal composition of the Co:Fe alloy that forms the focus of this study was 10:90. Additionally, CoFe films with a 70:30 composition were studied using polarized neutron reflectometry, and a 50:50 alloy was also studied by secondary ion mass spectrometry (SIMS). The RE:TM layers were grown on an underlayer of either Pt or W and then capped with either W or Pt, without breaking vacuum, giving layered structures with nominal thicknesses of either SiO_2 :Pt(7 nm)\GdCoFe(15 nm)\W(5 nm) or SiO_2 :W(5 nm)\GdCoFe(15 nm)\Pt(7 nm). The samples were magnetized in the film plane.

To explore any inhomogeneities and map the compositional and magnetic profiles through the film thickness, several complementary

experimental tools were utilized. Elemental profiling was undertaken using SIMS. Data were obtained by the bombardment of Cs^+ ions of 250 eV under optimized conditions to minimize any matrix effect. No charge neutralization method was applied. The magnetization profiles through the thickness for samples with different Gd contents were obtained from polarized neutron reflectometry (PNR) carried out on the POLREF beam line at the ISIS Neutron and Muon Source.⁶³ Measurements were undertaken at 10 and 700 mT for both polarizations of the neutron beam. Electron densities of the layers and interface widths, as well as the element-specific Gd magnetization profile through the sample thickness were obtained from analysis of x-ray resonant magnetic reflectivity (XRMR) measured on the XMaS Beamline at the ESRF.⁶⁴ XRMR was measured with circularly polarized x-rays tuned to the Gd L_3 edge (7.24 keV) with an in-plane magnetic field of ± 30 mT. The magnetization induced asymmetry in the measured XRMR signal was obtained from $\frac{I^+ - I^-}{I^+ + I^-}$, where I^+ and I^- denote the scattered intensity recorded under opposite magnetic saturation states using a fixed circular polarization. All measurements were undertaken at room temperature.

We first consider the results of the SIMS compositional profiling. Figure 1(a) shows the elemental profiles mapped through a Pt(7 nm)\Gd₂₃(Co₁₀Fe₉₀)₇₇(15 nm)\W(5 nm) trilayer. The analysis clearly identifies the Pt underlayer, the central GdCoFe layer, and the W capping layer. The slopes between the layers give an indication of the extent of the interfaces. It is clear that the interface of GdCoFe with Pt is wider than the interface with W. Significantly, the SIMS analysis demonstrates that the distributions of the Co, Fe, and Gd sublattices, atoms throughout the central layer are not uniform. The compositional inhomogeneity is more pronounced when the profiles are

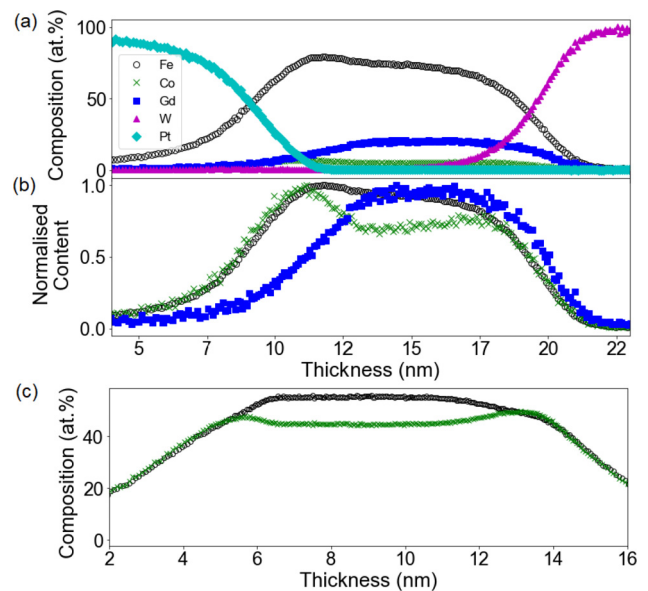


FIG. 1. (a) Secondary ion mass spectrometry profile of Pt(7 nm)\Gd₂₃(Co₁₀Fe₉₀)₇₇(15 nm)\W(5 nm) showing the elemental distribution through the trilayer. (b) Normalized elemental distributions of the Co, Fe, and Gd within the ferromagnetic alloy layer. (c) Elemental plot of Co and Fe through the thickness of a uniformly sputtered nominally 50:50 Co:Fe ferromagnetic layer of a W(5 nm)\Co₅₀Fe₅₀(14 nm)\Pt(7 nm) sample, for clarity the Pt and W are not shown.

normalized, see Fig. 1(b). Co and Fe have their highest concentration near the interface with Pt, while the Gd concentration increases rapidly from the interface with W to a broad peak within the center of the layer and gradually reduces over a longer lengthscale toward the bottom Pt interface. Thus, the RE:TM alloy has a higher TM content close to the Pt interface and an increased Gd concentration at the W interface. One interpretation of the interface compositional variation is due to chemical intermixing. However, it is known that Fe, Co, and Gd are all miscible with Pt;^{65–67} therefore, the different spatial variation of Co and Fe may be related to their higher electronegativity as compared to Gd. As W and Gd are immiscible,⁶⁷ the enhanced Gd concentration may simply reflect a reduced Co and Fe concentration resulting from enhanced Co and Fe at the Pt interface.

It is also interesting to observe that the Co and Fe distributions do not follow the same spatial trend. While both profiles peak close to the Pt interface, the distributions of Co and Fe through the layer are different. To better understand any impact of the RE and TM components on the compositional profile, a nominal 50:50 Co:Fe alloy with no RE was studied. The sample structure was W(5 nm)\Co₅₀Fe₅₀(14 nm)\Pt(7 nm), where W was the underlayer and Pt was on top, see Fig. 1(c). Away from the interfaces, the central part of the film has a uniform Co:Fe ratio of 45:55, but approaching both the Pt and W interfaces, the Co content increases to a small peak, the Fe content is reduced, and the Co:Fe ratio is then uniform within the interfaces. The Co peak at the Pt interface is slightly larger. The spatial variations in the composition within the alloys are expected to affect the resulting magnetic behavior, which is explored through scattering studies.

The changing Gd:Co:Fe ratio through the film thickness should result in local variations in the net magnetization, and the spatial profile of which was investigated using PNR. The nuclear scattering length density (structure) and magnetization profiles were obtained by fitting the neutron reflectivity data using the REF1D code (see the supplementary material).^{68,69} Since Gd has a high energy dependent neutron capture cross section, the data were fitted simultaneously to three separate wavelength ranges with different absorption. Figure 2 shows the reflectivity data for spin-up and spin-down polarized neutrons and the best fit simulations for samples with nominal alloy compositions of Gd₂₃(Co₇₀Fe₃₀)₇₇, Gd₈(Co₇₀Fe₃₀)₉₂, and Co₇₀Fe₃₀, respectively. Also

the best-fitting net magnetization profiles are shown. The Gd₂₃(Co₇₀Fe₃₀)₇₇ sample was designed to be close to magnetic compensation at room temperature, which is confirmed in the analysis with almost zero net magnetization through the layer thickness, see Fig. 2(a). In contrast, for the sample with 8% Gd content, the best fit shows the presence of a much larger magnetization throughout the Gd₈(Co₇₀Fe₃₀)₉₂ layer, but the profile is not uniform. The net magnetization is highest close the interface with W, approximately 8% lower at the Pt interface and falls by 11% of the maximum within the middle of the layer. A Gd-free Co₇₀Fe₃₀ sample showed a larger net magnetization overall, which is also non-uniform as expected, with the magnetization highest at the interface with the W and decreasing through the film thickness toward the Pt interface, see Fig. 2(c).

The PNR data clearly show that the net magnetization profile in all the samples is not uniform and is consistent with the compositional inhomogeneities observed with SIMS. However, as the RE and TM sub-lattices are both magnetic and knowing the problems of fitting neutron data for Gd-containing samples mentioned earlier, a correlation of the PNR data with SIMS compositional profiling was not attempted. Instead, in order to understand the relationship between the non-uniform compositional profile and the magnetization, the Gd compositional distribution was compared with the magnetization profile of the Gd sub-lattice through the alloy layer. Resonant x-ray reflectivity tuned to the Gd L₃ edge and using circular polarized light was measured to determine the Gd magnetization profile. XRMR allows simultaneous fitting of the structural and Gd-specific magnetic scattering length densities. The structural and magnetic asymmetry data were fitted using GenX. (Details are in the supplementary material.⁷⁰) The electron density (structure) and the Gd sub-lattice moment profile were determined for Pt(7 nm)\Gd₂₃(Co₁₀Fe₉₀)₇₇(15 nm)\W(5 nm). Figure 3(a) shows the specular reflectivity data with the best fit simulation while Fig. 3(b) shows the magnetic asymmetry data and the simultaneously fitted model for the Gd moment distribution. As seen in Fig. 3(c), the structural SLD shows the electronic density profile with the distinct Pt and W layers either side of GdCoFe and a spatially varying electron density within the GdCoFe layer from the Pt interface to the W layer. The magnetic scattering length profile shows the Gd magnetization through the layer. The Gd moment increases

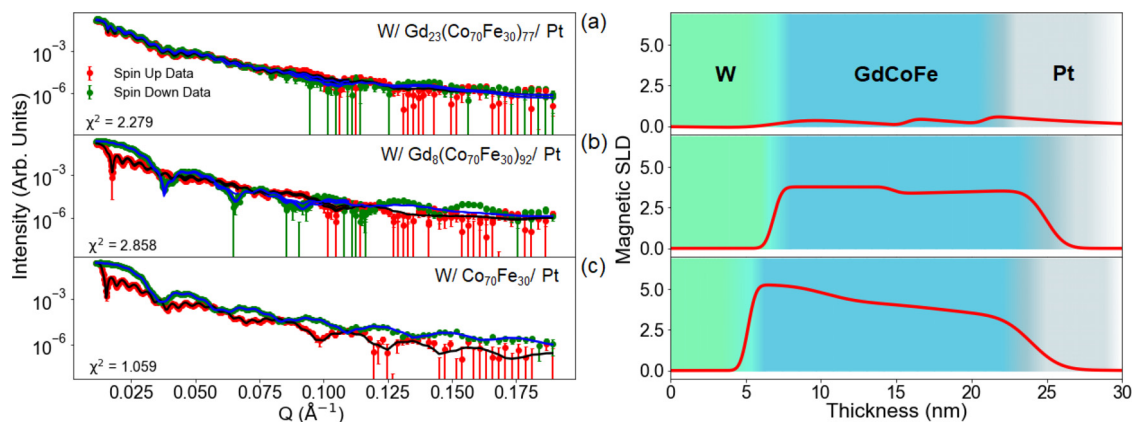


FIG. 2. Polarized neutron reflectivity measurements and best-fitting model simulations (left panel) and the resultant magnetic scattering length density profiles (right panel) for samples (a) W\Gd₂₃(Co₇₀Fe₃₀)₇₇\Pt, which is close to the magnetic compensation, (b) W\Gd₈(Co₇₀Fe₃₀)₉₂\Pt and (c) W\Co₇₀Fe₃₀\Pt, with no rare-earth content.

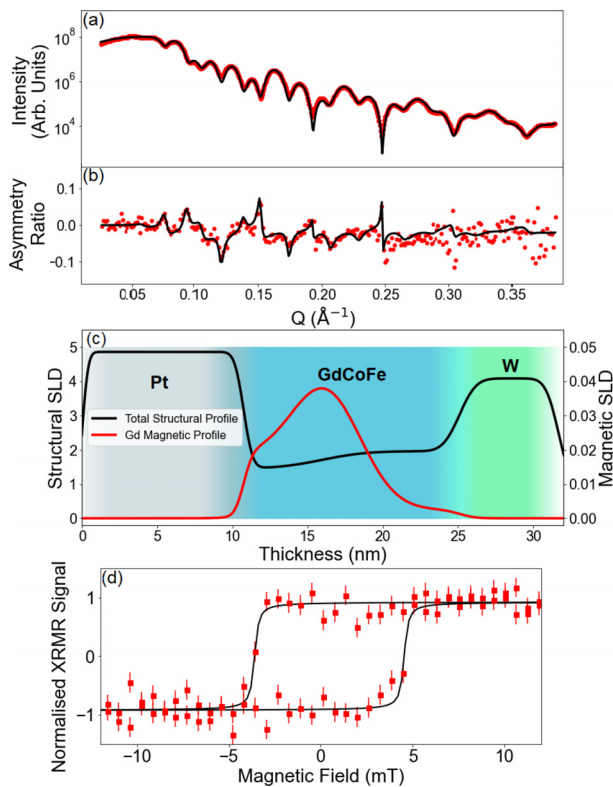


FIG. 3. (a) Resonant specular reflectivity data points and solid line showing best fitting simulation, (b) magnetic asymmetry ratio data points and the best fitting simulation. (c) Structural and magnetic SLD profiles for Pt/Gd₂₃(Co₁₀Fe₉₀)₇₇/W from the best fitting simulations. (d) Magnetic hysteresis from the Gd sub-lattice magnetic hysteresis showing a simple square loop of the soft ferrimagnetically coupled alloy.

rapidly from the Pt interface and then increases more slowly to a broad peak around the center of the GdCoFe layer, before decreasing approximately linearly to the W interface. By measuring the field dependence of $\frac{I^+ - I^-}{I^+ + I^-}$ at a fixed wave vector, $Q = 0.12 \text{ \AA}^{-1}$ magnetic hysteresis was obtained, see Fig. 3(c), which shows the Gd sub-lattice magnetic hysteresis showing a simple square loop of the soft ferrimagnetically coupled alloy.

All the collected data indicate the existence of compositional variations within the sputtered RE:TM and TM alloy films. XRMS and SIMS yielded magnetization and compositional profiles for Gd in the same Pt(7 nm)\Gd₂₃(Co₁₀Fe₉₀)₇₇/W(5 nm) sample that is plotted together in Fig. 4. The Gd moment largely follows the Gd distribution with the Gd moment largest in the center of the layer, corresponding to the highest Gd concentration. However, the behavior close to the interfaces is more complex and more susceptible to fitting uncertainties in the scattering data. Close to the Pt interface, the Gd moment is enhanced, which correlates with the peak in the Fe and Co contents (see Fe data in Fig. 4), while no enhancement occurs at the W interface when Fe and Co are lower. These data suggest that compositional variations change the local electronic environment of Gd, which, in turn, changes the Gd moment and, hence, the magnetization profile through the layer.

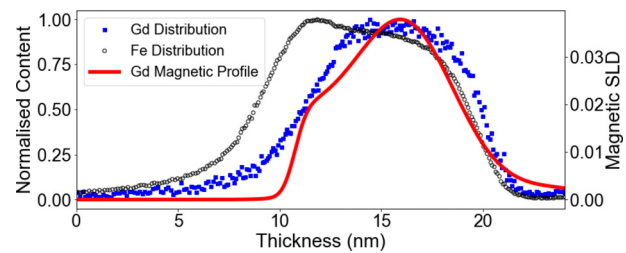


FIG. 4. Gd and Fe elemental profiles from SIMS combined with the Gd magnetic SLD profile from XRM through the same Pt(7 nm)\Gd₂₃(Co₁₀Fe₉₀)₇₇/W(5 nm) sample.

In conclusion, elemental mapping of nominally uniform ferrimagnetic alloy layers, typified by the Pt(7 nm)\GdCoFe(15 nm)\W(5 nm) structure, shows that the RE:TM ratio is not uniform, showing complex spatial variations that also depend on the elemental species of the under and over layers which in this case were Pt and W. The variations in composition influence both the Gd magnetization and the net magnetization profiles through the ferrimagnetic layer. These observations appear to be generic for sputtered films and have significant implications for the magnetic and spintronic behaviors of these alloys. Structurally, the Gd content determines the crystallinity/amorphicity of the RE:TM alloy. The amorphous state is critical for the development of a perpendicular magnetic anisotropy through the film. The RE:TM ratio also determines the net magnetization as well as both the magnetization and angular momentum compensation points. The local elemental distributions determine the magnetic structure and saturation magnetization locally through a layer, which, interestingly, for Gd is observed also to depend upon the Co and Fe concentration. Any compositional variations will lead to a distribution of compensation point temperatures throughout a film, broadening the compensation regime and impacting the magnetization and spintronic behavior such as domain wall dynamics and spin-orbit torque switching. Compositional variations at and across the interface would also directly impact spin transport and interface proximity-induced magnetization. The impact of compositional variations in these films needs to be considered more critically if ferrimagnetic alloy thin-films are to be integrated into future technologies.

See the supplementary material for information on the XRM and PNR data simulation.

We acknowledge funding from EPSRC for DR (No. EP/W524426/1) and from the Royal Society for DA (No. IF170030). We are grateful to EPSRC for X-ray beam time A28-1-1270 on XMaS, the UK CRG Beamline at the ESRF, and ISIS neutron source for the provision of beamtime RB2220266. We would like to thank Leon Bowen for the EDX measurements.

AUTHOR DECLARATIONS

Conflict of Interest

The authors have no conflicts to disclose.

Author Contributions

Oto-Obong Inyang: Conceptualization (equal); Data curation (equal); Formal analysis (equal); Investigation (equal); Methodology (equal);

Project administration (equal); Resources (equal); Software (equal); Visualization (equal); Writing – original draft (equal); Writing – review & editing (equal). **Del Atkinson:** Conceptualization (equal); Data curation (equal); Funding acquisition (equal); Methodology (equal); Resources (equal); Software (equal); Supervision (equal); Visualization (equal); Writing – original draft (equal); Writing – review & editing (equal). **Charles Swindells:** Conceptualization (equal); Data curation (equal); Formal analysis (equal); Investigation (equal); Methodology (equal); Resources (equal); Software (equal); Visualization (equal); Writing – original draft (equal); Writing – review & editing (equal). **Debi Rianto:** Data curation (equal); Formal analysis (equal); Investigation (equal); Software (equal); Writing – original draft (equal); Writing – review & editing (equal). **Laurence Bouchenoire:** Data curation (equal); Methodology (equal); Resources (equal); Software (equal); Writing – review & editing (equal). **Richard J. H. Morris:** Data curation (equal); Formal analysis (equal); Software (equal); Writing – review & editing (equal). **Alex Merkulov:** Data curation (equal); Formal analysis (supporting); Software (supporting); Writing – review & editing (equal). **Andrew Caruana:** Data curation (equal); Formal analysis (supporting); Software (equal); Writing – review & editing (equal). **Christy J. Kinane:** Data curation (equal); Formal analysis (equal); Software (equal); Writing – review & editing (equal). **Thomas Paul Ansem Hase:** Conceptualization (equal); Data curation (equal); Formal analysis (equal); Funding acquisition (equal); Methodology (equal); Software (equal); Supervision (equal); Writing – review & editing (equal).

DATA AVAILABILITY

The data that support the findings of this study are available from the corresponding author upon reasonable request. The ESRF and ISIS data are openly available in using ESRF at <https://data.esrf.fr/doi/10.1515/ESRF-DC-1301297694>, Ref. 72 and ISIS at <https://doi.org/10.5286/ISIS.E.RB2220266>, Ref. 73.

REFERENCES

- P. Chaudhari, J. Cuomo, and R. Gambino, “Amorphous metallic films for bubble domain applications,” *IBM J. Res. Develop.* **17**, 66–68 (1973).
- R. Hasegawa, R. Gambino, J. Cuomo, and J. Ziegler, “Effect of thermal annealing and ion radiation on the coercivity of amorphous Gd–Co films,” *J. Appl. Phys.* **45**, 4036–4040 (1974).
- R. Hasegawa, “Static bubble domain properties of amorphous Gd–Co films,” *J. Appl. Phys.* **45**, 3109–3112 (1974).
- S. Esho and S. Fujiwara, “Growth induced anisotropy in sputtered GdCo films,” *AIP Conf. Proc.* **34**, 331–333 (1976).
- R. Taylor and A. Gangulee, “Magnetization and magnetic anisotropy in evaporated GdCo amorphous films,” *J. Appl. Phys.* **47**, 4666–4668 (1976).
- A. Onton, N. Heiman, J. Suits, and W. Parrish, “Structure and magnetic anisotropy of amorphous Gd–Co films,” *IBM J. Res. Develop.* **20**, 409–411 (1976).
- H. Leamy and A. Dirks, “The microstructure of amorphous rare-earth/transition-metal thin films,” *J. Phys. D: Appl. Phys.* **10**, L95 (1977).
- N. Heiman, N. Kazama, D. Kyser, and V. Minkiewicz, “Effects of substrate bias and annealing on the properties of amorphous alloy films of Gd–Co, Gd–Fe, and Gd–Co–x (x = mo, cu, au),” *J. Appl. Phys.* **49**, 366–375 (1978).
- Y. Mimura, N. Imamura, T. Kobayashi, A. Okada, and Y. Kushiro, “Magnetic properties of amorphous alloy films of Fe with Gd, Tb, Dy, Ho, or Er,” *J. Appl. Phys.* **49**, 1208–1215 (1978).
- Y. Mimura, N. Imamura, and Y. Kushiro, “Hall effect in rare-earth–transition-metal amorphous alloy films,” *J. Appl. Phys.* **47**, 3371–3373 (1976).
- T. McGuire, R. Gambino, and R. Taylor, “Hall effect in amorphous thin-film magnetic alloys,” *J. Appl. Phys.* **48**, 2965–2970 (1977).
- T. Katayama, “Preparation and some magnetic properties of amorphous rare earth-transition metal films with perpendicular anisotropy for bubble memory,” *Microelectron. J.* **12**, 23–29 (1981).
- M. H. Kryder, “Magneto-optic recording technology,” *J. Appl. Phys.* **57**, 3913–3918 (1985).
- N. Imamura, S. Tanaka, F. Tanaka, and Y. Nagao, “Magneto-optical recording on amorphous films,” *IEEE Trans. Magn.* **21**, 1607–1612 (1985).
- H. Heitmann, M. Hartmann, M. Rosenkranz, and H. Tolle, “Amorphous rare earth-transition metal films for magneto-optical storage,” *Le J. de Phys. Colloques* **46**, C6-9 (1985).
- P. Hansen, C. Clausen, G. Much, M. Rosenkranz, and K. Witter, “Magnetic and magneto-optical properties of rare-earth transition-metal alloys containing Gd, Tb, Fe, Co,” *J. Appl. Phys.* **66**, 756–767 (1989).
- P. Hansen, “Magnetic amorphous alloys,” *Handbook Magn. Mater.* **6**, 289–452 (1991).
- J. Finley and L. Liu, “Spintronics with compensated ferrimagnets,” *Appl. Phys. Lett.* **116**, 110501 (2020).
- J. A. González, J. P. Andrés, and R. López Antón, “Applied trends in magnetic rare earth/transition metal alloys and multilayers,” *Sensors* **21**, 5615 (2021).
- S. K. Kim, G. S. Beach, K.-J. Lee, T. Ono, T. Rasing, and H. Yang, “Ferrimagnetic spintronics,” *Nat. Mater.* **21**, 24–34 (2022).
- R. K. Wangness, “Sublattice effects in magnetic resonance,” *Phys. Rev.* **91**, 1085 (1953).
- C. Stanciu, A. Kimel, F. Hansteen, A. Tsukamoto, A. Itoh, A. Kirilyuk, and T. Rasing, “Ultrafast spin dynamics across compensation points in ferrimagnetic GdFeCo: The role of angular momentum compensation,” *Phys. Rev. B* **73**, 220402 (2006).
- M. Binder, A. Weber, O. Mosendz, G. Woltersdorf, M. Izquierdo, I. Neudecker, J. Dahn, T. Hatchard, J.-U. Thiele, C. H. Back *et al.*, “Magnetization dynamics of the ferrimagnet cogd near the compensation of magnetization and angular momentum,” *Phys. Rev. B* **74**, 134404 (2006).
- N. Roschewsky, T. Matsumura, S. Cheema, F. Hellman, T. Kato, S. Iwata, and S. Salahuddin, “Spin-orbit torques in ferrimagnetic gdfeco alloys,” *Appl. Phys. Lett.* **109**, 112403 (2016).
- J. Finley and L. Liu, “Spin-orbit-torque efficiency in compensated ferrimagnetic cobalt-terbium alloys,” *Phys. Rev. Appl.* **6**, 054001 (2016).
- R. Mishra, J. Yu, X. Qiu, M. Motapothula, T. Venkatesan, and H. Yang, “Anomalous current-induced spin torques in ferrimagnets near compensation,” *Phys. Rev. Lett.* **118**, 167201 (2017).
- N. Roschewsky, C.-H. Lambert, and S. Salahuddin, “Spin-orbit torque switching of ultralarge-thickness ferrimagnetic GdFeCo,” *Phys. Rev. B* **96**, 064406 (2017).
- K. Ueda, M. Mann, P. W. De Brouwer, D. Bono, and G. S. Beach, “Temperature dependence of spin-orbit torques across the magnetic compensation point in a ferrimagnetic TbCo alloy film,” *Phys. Rev. B* **96**, 064410 (2017).
- J. Kim, D. Lee, K.-J. Lee, B.-K. Ju, H. C. Koo, B.-C. Min, and O. Lee, “Spin-orbit torques associated with ferrimagnetic order in Pt/GdFeCo/MgO layers,” *Sci. Rep.* **8**, 6017 (2018).
- T. Okuno, D.-H. Kim, S.-H. Oh, S. K. Kim, Y. Hirata, T. Nishimura, W. S. Ham, Y. Futakawa, H. Yoshikawa, A. Tsukamoto *et al.*, “Spin-transfer torques for domain wall motion in antiferromagnetically coupled ferrimagnets,” *Nat. Electron.* **2**, 389–393 (2019).
- K.-J. Kim, S. K. Kim, Y. Hirata, S.-H. Oh, T. Tono, D.-H. Kim, T. Okuno, W. S. Ham, S. Kim, G. Go *et al.*, “Fast domain wall motion in the vicinity of the angular momentum compensation temperature of ferrimagnets,” *Nat. Mater.* **16**, 1187–1192 (2017).
- S. A. Siddiqui, J. Han, J. T. Finley, C. A. Ross, and L. Liu, “Current-induced domain wall motion in a compensated ferrimagnet,” *Phys. Rev. Lett.* **121**, 057701 (2018).
- L. Caretta, M. Mann, F. Büttner, K. Ueda, B. Pfau, C. M. Günther, P. Hessler, A. Churikova, C. Klose, M. Schneider *et al.*, “Fast current-driven domain walls and small skyrmions in a compensated ferrimagnet,” *Nat. Nanotechnol.* **13**, 1154–1160 (2018).

- ³⁴Y. Hirata, D.-H. Kim, S. K. Kim, D.-K. Lee, S.-H. Oh, D.-Y. Kim, T. Nishimura, T. Okuno, Y. Futakawa, H. Yoshikawa *et al.*, “Vanishing skyrmion Hall effect at the angular momentum compensation temperature of a ferrimagnet,” *Nat. Nanotechnol.* **14**, 232–236 (2019).
- ³⁵N. Bergeard, A. Mougin, M. Izquierdo, E. Fonda, and F. Sirotti, “Correlation between structure, electronic properties, and magnetism in $\text{Co}_x\text{Gd}_{1-x}$ thin amorphous films,” *Phys. Rev. B* **96**, 064418 (2017).
- ³⁶V. Kudin, S. Rozouvan, and V. Staschuk, “Surface structure of $\text{Gd}_{20}\text{Co}_{80}$ alloy,” *Semicond. Phys., Quantum Electron. Optoelectron.* **24**, 56–63 (2021).
- ³⁷A. Chanda, J. Shoup, N. Schulz, D. Arena, and H. Srikanth, “Tunable competing magnetic anisotropies and spin reconfigurations in ferrimagnetic $\text{Fe}_{100-x}\text{Gd}_x$ alloy films,” *Phys. Rev. B* **104**, 094404 (2021).
- ³⁸G. Sala, C.-H. Lambert, S. Finizio, V. Raposo, V. Krizakova, G. Krishnaswamy, M. Weigand, J. Raabe, M. D. Rossell, E. Martinez *et al.*, “Asynchronous current-induced switching of rare-earth and transition-metal sublattices in ferrimagnetic alloys,” *Nat. Mater.* **21**, 640–646 (2022).
- ³⁹E. Kirk, C. Bull, S. Finizio, H. Sepehri-Amin, S. Wintz, A. K. Suszka, N. S. Bingham, P. Warnicke, K. Hono, P. Nutter *et al.*, “Anisotropy-induced spin reorientation in chemically modulated amorphous ferrimagnetic films,” *Phys. Rev. Mater.* **4**, 074403 (2020).
- ⁴⁰Z. Zheng, Y. Zhang, V. Lopez-Dominguez, L. Sánchez-Tejerina, J. Shi, X. Feng, L. Chen, Z. Wang, Z. Zhang, K. Zhang *et al.*, “Field-free spin-orbit torque-induced switching of perpendicular magnetization in a ferrimagnetic layer with a vertical composition gradient,” *Nat. Commun.* **12**, 1–9 (2021).
- ⁴¹O. Inyang, A. Rafiq, C. Swindells, S. Ali, and D. Atkinson, “The role of low Gd concentrations on magnetisation behaviour in rare earth: Transition metal alloy films,” *Sci. Rep.* **10**, 9767 (2020).
- ⁴²F. Hellman, A. Hoffmann, Y. Tserkovnyak, G. S. Beach, E. E. Fullerton, C. Leighton, A. H. MacDonald, D. C. Ralph, D. A. Arena, H. A. Dürr *et al.*, “Interface-induced phenomena in magnetism,” *Rev. Mod. Phys.* **89**, 025006 (2017).
- ⁴³T. J. Zega, A. T. Hanbicki, S. C. Erwin, I. Žutić, G. Kioseoglou, C. H. Li, B. T. Jonker, and R. M. Stroud, “Determination of interface atomic structure and its impact on spin transport using z-contrast microscopy and density-functional theory,” *Phys. Rev. Lett.* **96**, 196101 (2006).
- ⁴⁴J.-C. Rojas-Sánchez, N. Reyren, P. Laczkowski, W. Savero, J.-P. Attané, C. Deranlot, M. Jamet, J.-M. George, L. Vila, and H. Jaffrès, “Spin pumping and inverse spin hall effect in platinum: The essential role of spin-memory loss at metallic interfaces,” *Phys. Rev. Lett.* **112**, 106602 (2014).
- ⁴⁵C. Swindells, A. Hindmarch, A. Gallant, and D. Atkinson, “Spin transport across the interface in ferromagnetic/nonmagnetic systems,” *Phys. Rev. B* **99**, 064406 (2019).
- ⁴⁶K. Gupta, R. J. Wesselink, R. Liu, Z. Yuan, and P. J. Kelly, “Disorder dependence of interface spin memory loss,” *Phys. Rev. Lett.* **124**, 087702 (2020).
- ⁴⁷V. P. Amin and M. D. Stiles, “Spin transport at interfaces with spin-orbit coupling: Formalism,” *Phys. Rev. B* **94**, 104419 (2016).
- ⁴⁸L. Zhu, D. Ralph, and R. Buhrman, “Spin-orbit torques in heavy-metal-ferromagnet bilayers with varying strengths of interfacial spin-orbit coupling,” *Phys. Rev. Lett.* **122**, 077201 (2019).
- ⁴⁹H. T. Nembach, J. M. Shaw, M. Weiler, E. Jué, and T. J. Silva, “Linear relation between Heisenberg exchange and interfacial Dzyaloshinskii-Moriya interaction in metal films,” *Nat. Phys.* **11**, 825–829 (2015).
- ⁵⁰R. M. Rowan-Robinson, A. Stashkevich, Y. Roussigné, M. Belmuguenai, S.-M. Chérif, A. Thiaville, T. Hase, A. Hindmarch, and D. Atkinson, “The interfacial nature of proximity-induced magnetism and the Dzyaloshinskii-Moriya interaction at the Pt/Co interface,” *Sci. Rep.* **7**, 16835 (2017).
- ⁵¹X. Ma, G. Yu, C. Tang, X. Li, C. He, J. Shi, K. L. Wang, and X. Li, “Interfacial Dzyaloshinskii-Moriya interaction: Effect of 5d band filling and correlation with spin mixing conductance,” *Phys. Rev. Lett.* **120**, 157204 (2018).
- ⁵²R. White and D. Friedman, “Theory of the magnetic proximity effect,” *J. Magn. Mater.* **49**, 117–123 (1985).
- ⁵³P. Manna and S. Yusuf, “Two interface effects: Exchange bias and magnetic proximity,” *Phys. Rep.* **535**, 61–99 (2014).
- ⁵⁴O. Inyang, L. Bouchenoire, B. Nicholson, M. Tokaç, R. Rowan-Robinson, C. Kinane, and A. Hindmarch, “Threshold interface magnetization required to induce magnetic proximity effect,” *Phys. Rev. B* **100**, 174418 (2019).
- ⁵⁵C. Swindells, B. Nicholson, O. Inyang, Y. Choi, T. Hase, and D. Atkinson, “Proximity-induced magnetism in Pt layered with rare-earth-transition-metal ferrimagnetic alloys,” *Phys. Rev. Res.* **2**, 033280 (2020).
- ⁵⁶M. Caminale, A. Ghosh, S. Auffret, U. Ebels, K. Ollefs, F. Wilhelm, A. Rogalev, and W. Bailey, “Spin pumping damping and magnetic proximity effect in Pd and Pt spin-sink layers,” *Phys. Rev. B* **94**, 014414 (2016).
- ⁵⁷C. Swindells, H. Głowiński, Y. Choi, D. Haskel, P. Michałowski, T. Hase, P. Kuświk, and D. Atkinson, “Proximity-induced magnetism and the enhancement of damping in ferromagnetic/heavy metal systems,” *Appl. Phys. Lett.* **119**, 152401 (2021).
- ⁵⁸C. Swindells, H. Głowiński, Y. Choi, D. Haskel, P. Michałowski, T. Hase, F. Stobiecki, P. Kuświk, and D. Atkinson, “Magnetic damping in ferromagnetic/heavy-metal systems: The role of interfaces and the relation to proximity-induced magnetism,” *Phys. Rev. B* **105**, 094433 (2022).
- ⁵⁹H. Yang, A. Thiaville, S. Rohart, A. Fert, and M. Chshiev, “Anatomy of Dzyaloshinskii-Moriya interaction at Co/Pt interfaces,” *Phys. Rev. Lett.* **115**, 267210 (2015).
- ⁶⁰L. Zhu, D. C. Ralph, and R. A. Buhrman, “Maximizing spin-orbit torque generated by the spin Hall effect of Pt,” *Appl. Phys. Rev.* **8**, 031308 (2021).
- ⁶¹S. Jaiswal, K. Litzius, I. Lemesch, F. Büttner, S. Finizio, J. Raabe, M. Weigand, K. Lee, J. Langer, B. Ocker *et al.*, “Investigation of the Dzyaloshinskii-Moriya interaction and room temperature skyrmions in W/CoFeB/MgO thin films and microwires,” *Appl. Phys. Lett.* **111**, 022409 (2017).
- ⁶²K. Garello, F. Yasin, S. Couet, L. Souriau, J. Swerts, S. Rao, S. Van Beek, W. Kim, E. Liu, S. Kundu *et al.*, “Sot-MRAM 300 nm integration for low power and ultrafast embedded memories,” in *2018 IEEE Symposium on VLSI Circuits (IEEE, 2018)*, pp. 81–82.
- ⁶³See <https://www.isis.stfc.ac.uk/Pages/polref.aspx> for Polref Beamline (2020), accessed on June 20, 2023.
- ⁶⁴O. Bikondoa, L. Bouchenoire, S. D. Brown, P. B. J. Thompson, D. Wermeille, C. A. Lucas, M. J. Cooper, and T. P. A. Hase, “Xmas @ the ESRF,” *Phil. Trans. R. Soc. A* **377**, 20180237 (2019).
- ⁶⁵Y. Bao, A. Pakhomov, and K. M. Krishnan, “A general approach to synthesis of nanoparticles with controlled morphologies and magnetic properties,” *J. Appl. Phys.* **97**, 10J317 (2005).
- ⁶⁶H. Berg and J. Cohen, “Long-range order and ordering kinetics in CoPt_s ,” *Metallurgical Mater. Trans. B* **3**, 1797–1805 (1972).
- ⁶⁷R. Zhang, X. Kong, H. Wang, S. Zhang, D. Legut, S. Sheng, S. Srinivasan, K. Rajan, and T. C. Germann, “An informatics guided classification of miscible and immiscible binary alloy systems,” *Sci. Rep.* **7**, 1–12 (2017).
- ⁶⁸P. Kienzle, B. Maranville, K. O’Donovan, J. Ankner, N. Berk, and C. Majkrzak, <https://www.nist.gov/ncnr/reflectometry-software> (2017), accessed on September 28, 2021.
- ⁶⁹P. Kienzle, J. Krycka, N. Patel, and I. Sahin, <https://bumps.readthedocs.io/en/latest/> (2011), accessed on September 28, 2021.
- ⁷⁰M. Björck and G. Andersson, “Genx: An extensible x-ray reflectivity refinement program utilizing differential evolution,” *J. Appl. Crystallogr.* **40**, 1174–1178 (2007).
- ⁷¹K. A. Thórarinsdóttir, T. Hase, B. Hjörvarsson, and F. Magnus, “Amorphous exchange-spring magnets with crossed perpendicular and in-plane anisotropies,” *Phys. Rev. B* **103**, 014440 (2021).
- ⁷²D. Atkinson, T. Hase, C. Swindells, O.-O. Inyang, and L. Bouchenoire (2023), “Fundamental magnetism and future technology: Mapping proximity magnetism in W and Pt layered with Rare-Earth/Transition-Metal ferrimagnets through the compensation temperature,” ESRF. <https://data.esrf.fr/doi/10.15151/ESRF-DC-1301297694>
- ⁷³C. Swindells, D. Rianto, D. Atkinson, A. Caruana, O.-O. Inyang, and T. Hase (2022), “Understanding the non-uniform Gd distribution in rare earth: Transition metal ferrimagnetic alloys for spintronics applications,” ISIS. <https://doi.org/10.5286/ISIS.E.RB2220266>